Available online at www.sciencedirect.com
SCIENCE DIRECT®
Developmental Biology 265 (2004) 246–261
DEVELOPMENTAL BIOLOGY
www.elsevier.com/locate/ydbio

Transcription factor Ap-2α is necessary for development of embryonic melanophores, autonomic neurons and pharyngeal skeleton in zebrafish

Erin K. O'Brien,[a] Claudia d'Alençon,[b] Gregory Bonde,[b] Wei Li,[b] Jeff Schoenebeck,[c] Miguel L. Allende,[d] Bruce D. Gelb,[e] Deborah Yelon,[c] Judith S. Eisen,[f] and Robert A. Cornell[b,*]

[a] *Department of Otolaryngology, University of Iowa College of Medicine, Iowa City, IA 52242, USA*
[b] *Department of Anatomy and Cell Biology, University of Iowa College of Medicine, Iowa City, IA 52242, USA*
[c] *Departamento de Biología, Facultad de Ciencias, Universidad de Chile, Santiago, Chile*
[d] *Developmental Genetics Program, Skirball Institute of Biomolecular Medicine, New York University School of Medicine, New York, NY 10016, USA*
[e] *Departments of Pediatrics and Human Genetics, Mount Sinai School of Medicine, New York, NY 10029, USA*
[f] *Institute of Neuroscience, University of Oregon, Eugene, OR 97403, USA*

Received for publication 3 April 2003, revised 25 September 2003, accepted 25 September 2003

Abstract

The genes that control development of embryonic melanocytes are poorly defined. Although transcription factor Ap-2α is expressed in neural crest (NC) cells, its role in development of embryonic melanocytes and other neural crest derivatives is unclear because mouse *Ap-2α* mutants die before melanogenesis. We show that zebrafish embryos injected with morpholino antisense oligonucleotides complementary to *ap-2α* (*ap-2α* MO) complete early morphogenesis normally and have neural crest cells. Expression of *c-kit*, which encodes the receptor for the Steel ligand, is reduced in these embryos, and, similar to zebrafish *c-kit* mutant embryos, embryonic melanophores are reduced in number and migration. The effects of *ap-2α* MO injected into heterozygous and homozygous *c-kit* mutants support the notion that Ap-2α works through C-kit and additional target genes to mediate melanophore cell number and migration. In contrast to *c-kit* mutant embryos, in *ap-2α* MO-injected embryos, melanophores are small and under-pigmented, and unexpectedly, analysis of mosaic embryos suggests Ap-2α regulates melanophore differentiation through cell non-autonomous targets. In addition to melanophore phenotypes, we document reduction of other neural crest derivatives in *ap-2α* MO-injected embryos, including jaw cartilage, enteric neurons, and sympathetic neurons. These results reveal that Ap-2α regulates multiple steps of melanophore development, and is required for development of other neuronal and non-neuronal neural crest derivatives.

Keywords: Transcription factor *ap-2*; Zebrafish; Morpholino; Neural crest; Melanocyte; Branchial arches; Cranial nerves; *c-kit*; Enteric neurons; Sympathetic neurons; Hirschsprung's disease

Introduction

Various growth factors are known to regulate the multiple steps of melanocyte development, but cell-autonomous requirements for melanocyte development are less well defined. For instance, misexpression and loss-of-function studies in zebrafish suggest Wnt signaling directs neural crest cells to adopt the melanophore fate (Dorsky et al., 1998). Analysis of mouse and zebrafish mutants suggest that steel factor (SCF), mediated by its receptor Kit, controls melanoblast migration and proliferation (Brannan et al., 1991; Nocka et al., 1989, 1990; Parichy et al., 1999; Reith et al., 1990; Tan et al., 1990). The ligand endothelin-3, working through its receptor Ednrb, also appears to promote melanoblast proliferation and perhaps differentiation (Baynash et al., 1994; Lahav et al., 1996; Reid et al., 1996; Shin et al., 1999). In mice, α-melanocyte-stimulating hormone

* Corresponding author. Department of Anatomy and Cell Biology, University of Iowa College of Medicine, 1-532 BSB, Iowa City, IA 52242. Fax: +1-319-335-7198.
E-mail address: robert-cornell@uiowa.edu (R.A. Cornell).

0012-1606/$ - see front matter © 2003 Elsevier Inc. All rights reserved.
doi:10.1016/j.ydbio.2003.09.029

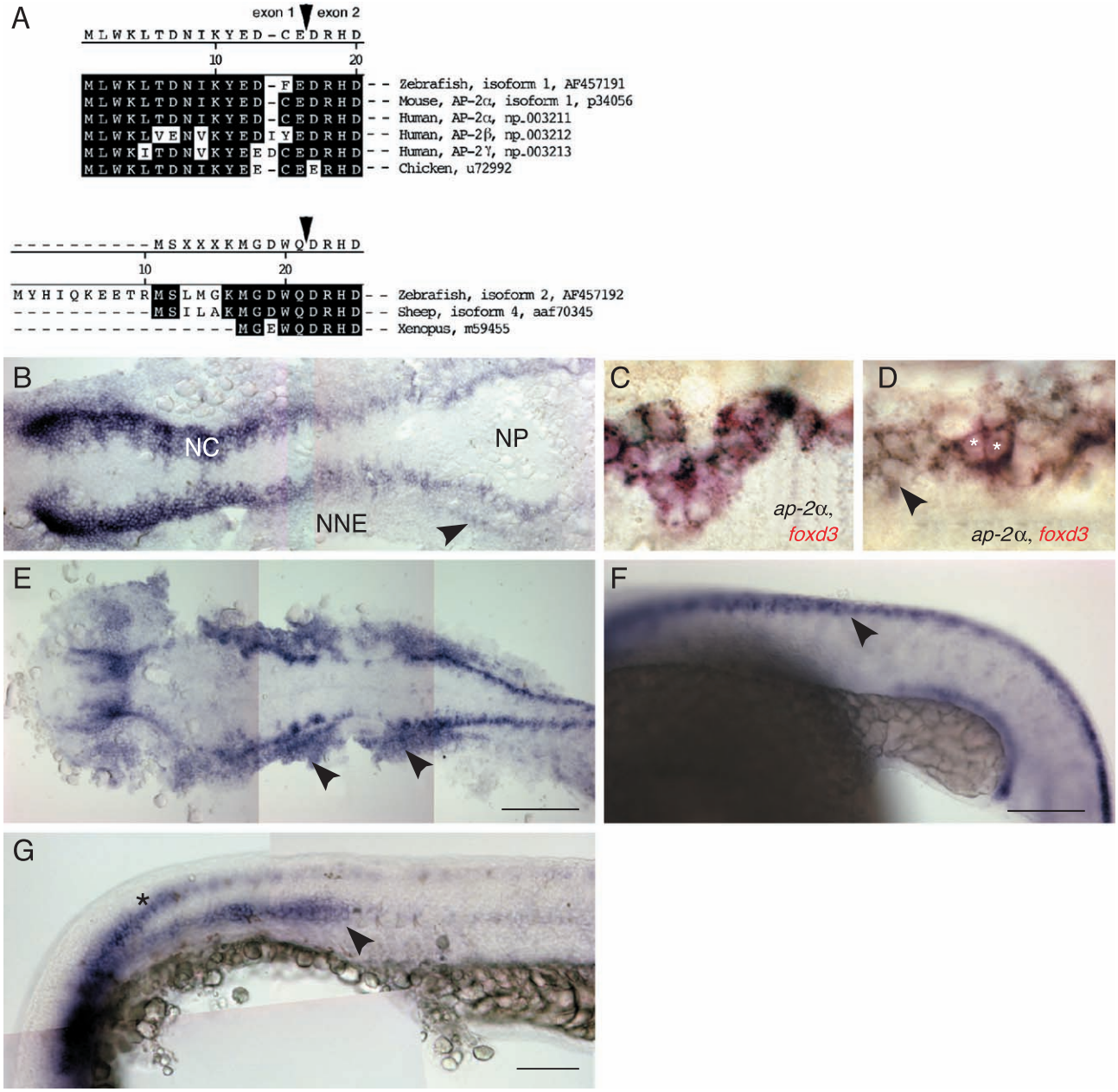

Fig. 1. Gene structure of *ap-2α* and its expression in neural crest. (A) Multi-species comparison of predicted peptide sequence of exon 1 of AP-2 proteins. (Top) Exon 1, zebrafish Ap-2α, isoform 1 (GenBank accession number , AF457191) differs by just 1 of 15 amino acids from human AP-2α (NP_003211) (Williams et al., 1988) and mouse Ap-2α isoform 1 (P34056) (Moser et al., 1993), which are identical. Genbank accession number of each gene is included. The amino terminal sequence of zebrafish Ap-2α isoform 1 is also highly conserved in human AP-2β, AP-2γ, and AP-2δ, as well as in rat and chicken AP-2 proteins. (Bottom) Zebrafish Ap-2 isoform 2 (AF457192) differs from isoform 1 by an alternative exon 1, but utilizes the same exons 2–7. Exon 1 of isoform 2 shows no significant homology to known mouse or human isoforms, but shares 8 of 11 amino acids in sheep AP-2α, variant 6 (GenBank accession number , AAF70345) (Limesand and Anthony, 2001) and four of five amino acids with frog AP-2 (Winning et al., 1991). (B–H) Expression of *ap-2α* RNA revealed by whole mount in situ hybridization using a probe complementary to full-length *ap-2α,* isoform 1. Under the hybridization conditions employed here, this probe will hybridize to isoform 2 and any other first-exon variants of *ap-2α*. Anterior is to the left in all panels. (B) Dorsal view of a flat-mounted embryo at 12 hpf. High-level expression was evident in premigratory neural crest (NC) and pronephros (arrowhead), and low-level expression was present in non-neural ectoderm (NNE). Expression was absent from neural plate (NP). (C) Dorsal view of the anterior trunk lateral neural plate, of an 11 hpf, flat-mounted embryo, processed to reveal *ap-2α* RNA, in blue, and *foxd3* RNA, a marker of premigratory neural crest (Odenthal and Nusslein-Volhard, 1998), in red. All *foxd3*-expressing cells in lateral neural plate also expressed *ap-2α,* supporting the notion that these cells are premigratory neural crest (PNC). (D) The same embryo as shown in C, but focused in more caudal lateral neural plate. At this axial level, some lateral neural plate cells, presumed to be PNC, expressing *ap-2α* also expressed *foxd3* (asterisks) and others did not yet express *foxd3* (arrowhead), suggesting *ap-2α* is expressed in PNC before *foxd3*. (E) Dorsal head view and (F) lateral trunk view of embryos at 17 hpf. Expression was evident lateral to the midbrain and hindbrain, in presumed migrating cranial neural crest (arrowheads in E), and in dorsal neural tube, in trunk neural crest (arrowhead in F). (G) Lateral view trunk of 24-hpf embryo. Expression was detected in the migrating posterior lateral line primordium (arrowhead) and in interneurons of the hindbrain (asterisk) and trunk, but was absent from trunk neural crest by this stage. All scale bars, 100 μm.

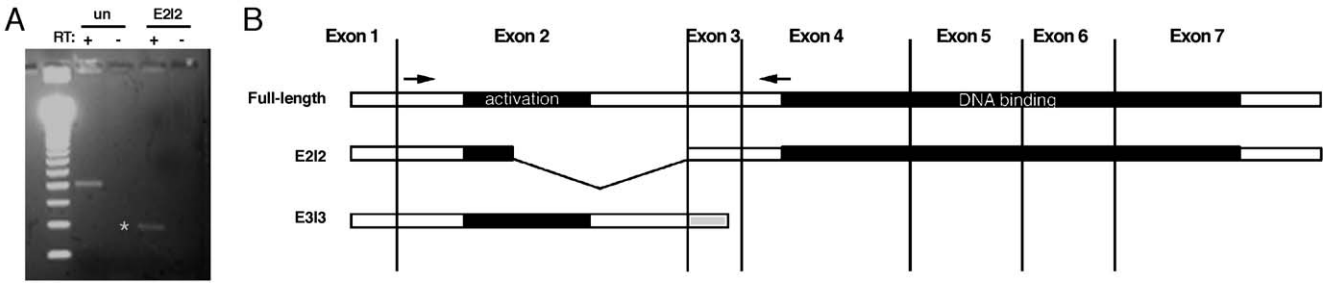

Fig. 2. Morpholinos disrupt splicing of *ap-2α* mRNA. RNA was harvested at 18 hpf from 50 uninjected control embryos (un), or 50 embryos injected at the 1–4 cell stage with 2–5 nl of 1 mg/ml *ap2* E2I2 morpholino (MO) (*ap-2α* MO embryos), and cDNA was synthesized. Nonquantitative polymerase chain reaction was carried out using a forward primer in exon 2 and a reverse primer in exon 4 of *ap-2α*. (A) *ap-2α* PCR products, separated by gel electrophoresis and stained with ethidium bromide. Amplification of cDNA from uninjected embryos (un) yielded a single band of the expected size of 482 bp, while amplification of cDNA from *ap-2α* MO embryos (MO) yielded a smaller band of 245 bp (asterisk), as well as the full-length band of 482 bp (not visible in this exposure). (– RT) Negative-control reactions run in parallel, where reverse transcriptase was omitted from the cDNA synthesis reactions. (B) Schematic diagram of Ap-2α proteins, resulting from (top) normal *ap-2α* transcript (isoform 1), and from the principal alternate transcripts induced by *ap-2α* E2I2 and *ap-2α* E3I3 morpholinos. Approximate position of boundaries of exons 1–7 are indicated (deduced from ctg25479), and the approximate limits of the activation domain and the DNA binding domain are also indicated (from Wankhade et al., 2000). Arrows in B indicate approximate locations of the primers used for PCR amplification of cDNA. (middle) Structure of the predicted protein encoded by the principal alternate transcript induced by the E2I2 MO. Sequence analysis of the 245-bp band from E2I2 MO embryos suggests it resulted from a transcript in which exon 3 was ligated to a site within exon 2. The encoded protein is missing 79 amino acids of exon 2 (amino acids 76–155 of Ap-2α, isoform 1), including most of the predicted activation domain (Wankhade et al., 2000). While this protein may function as a dominant negative, its low levels of expression (i.e., lower than that of endogenous levels of Ap-2α) make it unlikely to exert a profound effect on other homologues of *ap-2*. (bottom) Structure of the predicted protein encoded by the principal alternate transcript induced by the E3I3 MO. PCR amplification of *ap-2α* cDNA, using the same primers as above, from E3I3-MO-injected embryos also revealed one major alternate transcript (not shown). Sequence analysis of the PCR product showed that it resulted from a transcript in which exon 4 was fused to exon 2. This abnormal junction leads to a shift of the open reading and the appearance of an in-frame stop codon 10 amino acids after the end of exon 2. The protein encoded by such a transcript would contain nothing more than an activation domain, and is thus likely to be entirely nonfunctional.

regulates the type of melanin that is produced, although the role of this hormone in human pigmentation is unclear (Voisey and van Daal, 2002).

What are the early cell autonomous requirements for the melanocyte fate? The transcription factor Microphthalmia (Mitf) is among the earliest known markers of the melanoblast fate, and is required for melanocyte development (reviewed in Tachibana, 2000). Other candidates for such genes include transcription factors that are expressed from early stages in neural crest, including activating protein 2 (*AP-2*). There are four member of the *AP-2* family in humans and mice (α, β, γ, and more diverged δ) (reviewed in Hilger-Eversheim et al., 2000; see Zhao et al., 2001). To date, only one homologue each, most closely resembling mammalian *AP-2α*, has been characterized in zebrafish, frog, lamprey, amphioxus, and fruit fly (Bauer et al., 1998; Furthauer et al., 1997; Meulemans and Bronner-Fraser, 2002; Winning et al., 1991). In vertebrates, *AP-2* homologues (except *AP-2δ*) are expressed in the epidermis and neural plate border and later in migrating neural crest (NC) cells at all axial levels (Chazaud et al., 1996; Furthauer et al., 1997; Luo et al., 2002; Meulemans and Bronner-Fraser, 2002; Mitchell et al., 1991; Moser et al., 1997; Zhao et al., 2001). In cephalochordates (e.g., *Amphioxus*), which are thought to have separated from the vertebrate lineage before the appearance of neural crest, *Ap-2* is expressed in non-neural ectoderm but not in the dorsal neural tube (Meulemans and Bronner-Fraser, 2002).

Ap-2α influences the fate of melanoma cells; however, a role for Ap-2α in development of melanocytes has not been adequately tested. Huang et al. (1998) showed that levels of *AP-2α* and *KIT* are reduced in aggressive but not non-aggressive melanoma cells. Misexpression of *AP-2α* in aggressive melanoma led to increased levels of *KIT* and decreased tumorigenicity and metastatic potential (Huang et al., 1998). These results suggest that AP-2α would regulate *KIT* expression in embryonic melanocytes as well. Mouse embryos homozygous for a targeted deletion of *Ap-2α* have defects in some neural crest derivatives, including jaw elements and cranial ganglia (Schorle et al., 1996; Zhang et al., 1996), and in vitro studies implicate Ap-2α in control of Schwann cell differentiation (Stewart et al., 2001). However, *Ap-2α* mutant embryos die at birth from severe morphological defects, thus melanocyte development could not be evaluated (Schorle et al., 1996; Zhang et al., 1996). To circumvent the requirement for Ap-2α in early morphogenesis, Nottoli et al. (1998) created mosaic embryos from wild-type and *Ap-2α* mutant cells. Of note, they reported that melanocytes derived from mutant cells with some frequency in these mosaics, but this experiment did not reveal population-level effects of Ap-2α on melanocytes. *X. laevis* embryos injected with antisense oligonucleotides targeting *AP-2* have reduced expression of neural crest markers, however, they stall in development shortly after gastrulation, thus they were not useful for evaluating a role for Ap-2α in neural crest patterning (Luo et al., 2002).

To establish a model system in which to further explore the requirement for Ap-2α in melanocytes and other neural crest derivatives, we injected morpholino antisense oligonucleotides (morpholinos) to knockdown the function of Ap-2α in zebrafish. Early development was normal in embryos injected with *ap-2α* morpholinos and neural crest was present, although expression of *crestin* in neural crest was reduced. Injected embryos developed with a reduced number of melanophores, and melanophores migrated and differentiated abnormally. Concomitant with these visible defects was a reduction of *c-kit* expression, which is known to be required for melanophore cell number and migration, and of *dopachrome tautomerse* (*dct*) expression, presumed to be necessary for melanophore differentiation. In addition to melanophore defects, we detected a reduction of jaw cartilage, sympathetic neurons, and enteric neurons. Analysis of zebrafish embryos deficient in Ap-2α has thus uncovered embryonic functions for this protein that were obscured in the more severely defective mouse and frog embryos lacking AP-2α.

Methods

Fish and embryo rearing

Zebrafish adults and embryos were reared as previously described (Westerfield, 1993) in the University of Iowa Zebrafish Facility and staged by hours or days post fertilization at 28.5°C (hpf or dpf) (Kimmel et al., 1995). Homozygous or heterozygous *sparse* mutant embryos, harboring a null allele of *c-kit* (*sparse*^{b5}) (Parichy et al., 1999), were generated by crossing homozygous adults to each other, or to wild-type adults, respectively.

Morpholino composition and injection

Morpholino antisense oligonucleotides (MO) (Gene Tools, Corvalis, OR) were designed to complement zebrafish *ap-2α*. The genomic structure of *ap-2α* was inferred from genomic traces and contigs found at , www.ensembl.org. Two isoforms of zebrafish AP-2 have been identified, which differ only by their first exon (Genbank accession numbers: , AF457191 and , AF457192, isoforms 1 and 2, respectively) (Furthauer et al., 1997). The first six exons, including the alternate first exons, are contained in contig ctg25479.

To target both isoforms simultaneously, we used *ap-2α* E2I2 MO (5′-AGCTTTTCTTCTTACCTGAACATCT-3′), which overlaps the exon2–intron2 splice site, or *ap-2α* E3I3 MO (5′-GAAATTGCTTACCTTTTTTGATTAC-3′), which overlaps the exon3–intron3 splice site. Negative controls included the standard random 25-mer from the supplier (Gene Tools), and a variant of *ap-2α* E2I2 MO, *ap-2α* E2I2 mismatch MO (5′-AGGTTATCTTGTCACCTCAAGATCT-3′) which has polymorphisms at six bases. Morpholinos were reconstituted in Danieux buffer (Nasevicius and Ekker, 2000), then diluted in 0.2 M KCl to 1 mg/ml (E2I2) or 4 mg/ml (E3/I3 and negative controls morpholinos). Embryos were injected with 2–4 nl of diluted morpholino at the 2–8 cell stage into the yolk immediately below the blastomeres. For all phenotypes reported here, at least 100 injected embryos were analyzed in three or more injection experiments. The reported phenotype was seen in at least 50% of embryos injected with either *ap-2α* E2I2 or *ap-2α* E3I3 MO at the indicated doses, except as noted in figure legends. When referred to in the text, the "strongly affected" phenotype was observed in 5–10% of embryos injected with E2I2 or E3I3 but never in embryos injected with control morpholinos.

RT-PCR

Fifteen embryos, either uninjected or injected with 2–4 nl of E2I2 MO at 1.0 mg/ml or E3I3 MO at 4.0 mg/ml, were quick-frozen to −80°C at 16 hpf, then RNA was harvested from them with RNAwiz (Ambion, Austin, TX). First-strand cDNA was synthesized with 200 ng of total RNA, 100 ng of random hexamer primers, 200 units of M-MLV Reverse Transcriptase (Invitrogen, Carlsbad, CA), 0.5 mM dNTPs, 50 mM Tris–HCl, pH 8.3, 75 mM KCl, 3 mM $MgCl_2$, 0.01 mM DTT, 40 units of Rnase Inhibitor, (Invitrogen), incubated at 37°C for 1 h. Nonquantitative polymerase chain reaction (PCR) was performed with 2.5 units of JumpStart Taq polymerase (Sigma, St. Louis, MO), 10 mM Tris–Hcl, pH 8.3, 50 mM KCl, 1,5 mM $MgCl_2$, 0.2 mM each dNTP, a forward primer in exon 2 (5′-CGCTCCTCCGCTGTCTCAT-3′), a reverse primer in exon 4 (5′-TCTAGATTCGGGTTTACCACACC-3′) (Xba1 restriction site added to the 5′ end), and 1/20 of the cDNA synthesis reaction. PCR was run on a thermal cycler (MJ Research, Waltham, MA), with the following program: 2 min at 94°C, followed by 35 rounds of 20 s at 92°C, 10 s at 94°C, 30 s at 60°C, and 30 s at 72°C, followed by a final round of 5 min at 72°C.

Gene expression analysis

DIG-labeled antisense RNA probes (Roche Diagnostics, Mannheim, Germany) for in situ hybridization were generated from plasmids as follows: *ap-2α*, (Furthauer et al., 1997), *Not*1/T7; *crestin*, (Rubinstein et al., 2000), *Not*1/T7; *c-kit* (Parichy et al., 1999), *Xho*1/T3; *dct*, (Kelsh et al., 1996), *Eco*R1/T7; *dlx2* (Akimenko et al., 1994), *Bam*H1/T7; *ednrb1*, (Parichy et al., 2000a), *Xho*1/T3; *foxd3* plasmid (*fkd6*—Zebrafish Information Network) (Odenthal and Nusslein-Volhard, 1998), *Bam*H1/T7; *mitf*, (Lister et al., 1999), *Eco*R1/T7; *sox10*, (Dutton et al., 2001b), *Sal*1/T7. Two-probe in situ analysis was conducted with *foxd3* probe synthesized using FITC-UTP and *ap-2α* synthesized using DIG-UTP (Roche Diagnostics). Embryos were hybridized

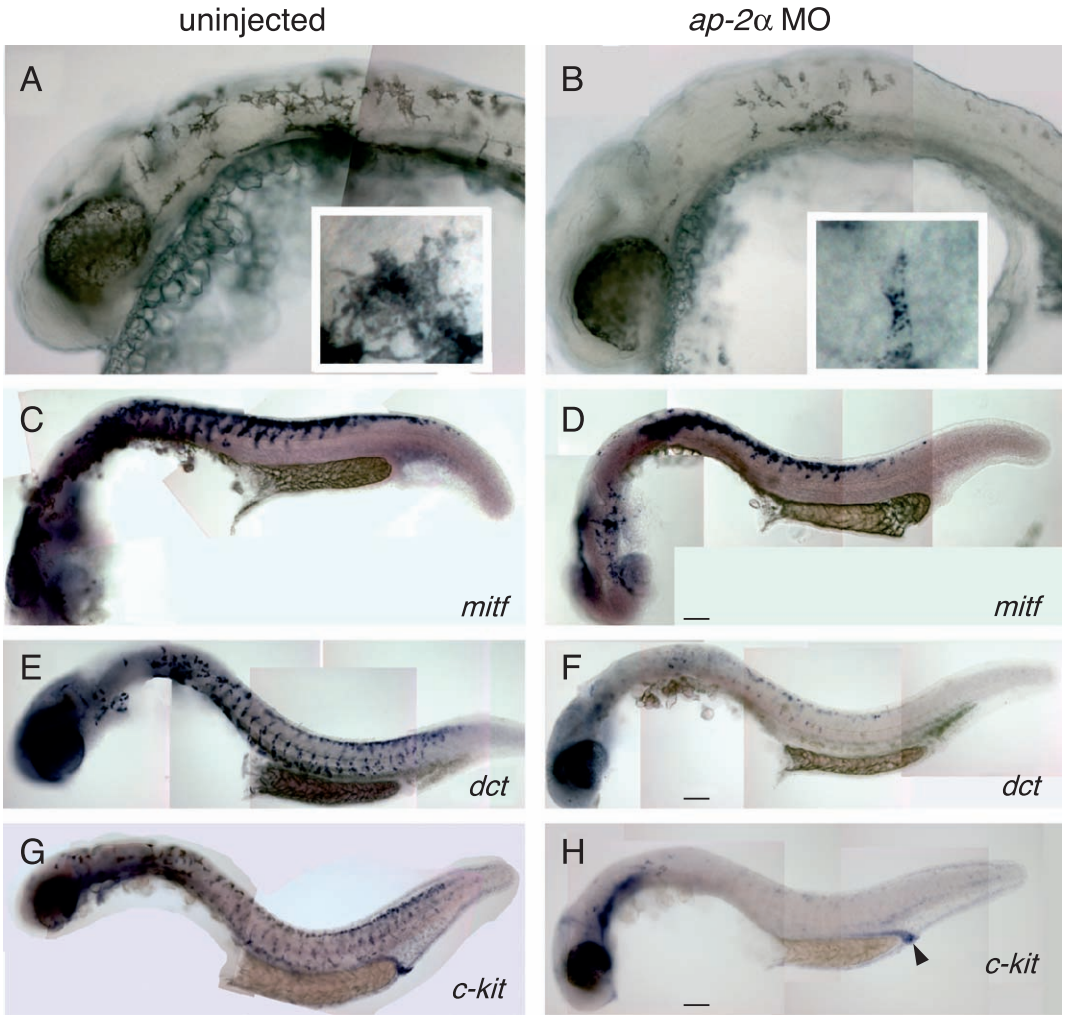

Fig. 3. Cell number, migration, and differentiation defects in embryonic melanophores in *ap-2α* MO embryos. (A and B) Lateral view of 30-hpf embryos. (A) Uninjected embryos had visible melanophores. (B) *ap-2α* MO embryos had a clearly reduced number of melanophores in the head and trunk regions. Insets, high-magnification views of single melanophores. Melanophores in *ap-2α* MO embryos were less pigmented (less black) and less dendritic than melanophores in the equivalent position in uninjected embryos. (C and D) Lateral view of embryos fixed at 22 hpf and processed to reveal *mitf*, which is expressed in melanophores and unmelanized melanoblasts and some other neural crest (Lister et al., 1999). (C) In uninjected embryos, *mitf* expressing cells were abundant. (D) In *ap-2α* MO embryos, melanoblasts were reduced in number, particularly in the trunk, and are clustered abnormally near dorsal neural tube. (E and F) Lateral views of embryos fixed at 28 hpf and processed to reveal *dct* expression. (E) In uninjected embryos, melanoblasts were seen throughout the trunk, while in (F) *ap-2α* MO embryos, their numbers were reduced, and expression was highly reduced within single cells. (G and H) Lateral view of embryos fixed at 24 hpf and processed to reveal *c-kit* expression in melanophores and melanoblasts (Parichy et al., 1999). (G) In uninjected embryos, *c-kit*-expressing melanophores and melanoblasts were abundant. (H) In *ap-2α* MO embryos, the number of melanoblasts and melanophores expressing *c-kit* was reduced, and the level of expression in individual cells was reduced, while expression near the anus was normal (arrowhead). All scale bars, 100 μm. Scale bar in D applies for both C and D, etc.

with *ap-2α* and *foxd3* probes simultaneously, washed, blocked, incubated in 1:15 000 dilution of anti-FITC conjugated to alkaline phosphatase, washed, and developed in Fast Red (Sigma product F-4648). Embryos were subsequently stripped of antibody by washing in 1% glycine, pH 2.0, 3× 10 min at RT, then reblocked, incubated in anti-DIG alkaline phosphatase, and developed as usual in NBT/BCIP (Roche).

Markers of trigeminal ganglia, used in whole mount prepartions, included Zn 12 (Metcalfe et al., 1990) and anti-Hu (Marusich et al., 1994) immunoreactivity at 28 hpf and 4 dpf respectively, and *ngn1* RNA expression at 18 hpf (Andermann et al., 2002; Korzh et al., 1998). Monoclonal antibodies were used at the following dilutions: zn12, 1:4000 (Metcalfe et al., 1990); and anti-HU (monoclonal antibody 16a11, Molecular Probes, Eugene, Oregon) (Marusich et al., 1994), 1:100. Whole mount samples were developed with horse radish peroxidase as described elsewhere (Cornell and Eisen, 2002).

Alcian green was used to label pharyngeal cartilage as described (Kimmel et al., 1998). Anti-tyrosine hydroxylase immunoreactivity just ventral to the dorsal aorta

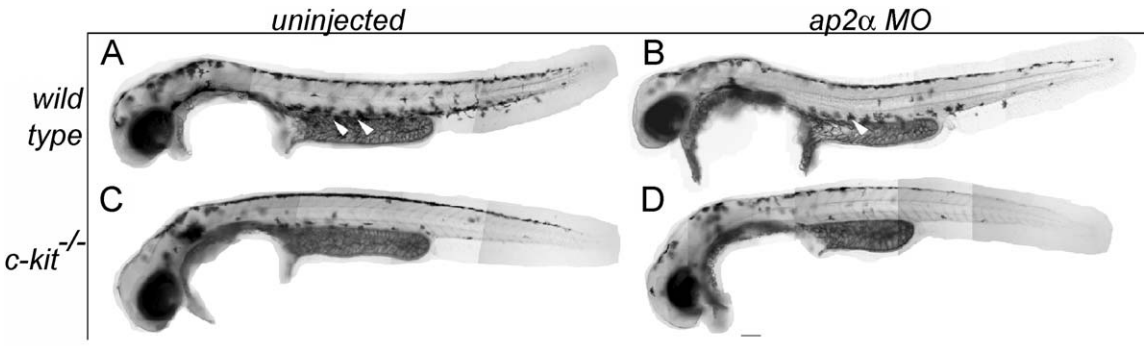

Fig. 4. Melanophore cell number and migration regulated by Ap-2α and C-kit. Lateral views of fixed embryos at 42 hpf. (A) Uninjected wild-type embryo and (B) *ap-2α* morpholino-injected wild-type embryo. *ap-2α* MO embryos had a significant reduction of the total number of melanophores (uninjected: 317.9 ± 23.5 total melanophores; *ap-2α* MO embryos: 120.6 ± 27.3 total melanophores; $n = 10$, $P < 0.0001$), and the fraction of them found in the ventral stripes (arrowheads) (uninjected: 45.6 ± 2.8%; *ap-2α* MO embryos: 27.3 ± 6.0%; $n = 10$, $P < 0.0001$). (C) Uninjected *c-kit* homozygous mutant embryos similarly have fewer total melanophores, with fewer migrated to the ventral stripe, than wild-type embryos (Parichy et al., 1999). (D) *c-kit* homozygous mutant embryos injected with *ap-2α* morpholino have still further melanophores than uninjected *c-kit* homozygous mutant embryos (*c-kit* mutants: 196 ± 23.3 melanophores, *ap-2α* MO injected *c-kit* mutants: 69.4 ± 24.1 melanophores, $n = 10$ embryos, $P < 0.0001$), and a smaller fraction in ventral stripes (*c-kit* mutants: 13.2 ± 3.2%, *ap-2α* MO *c-kit* mutants: 8.3 ± 4.4%, $n = 10$ embryos, $P < 0.01$). Scale bar, 100 μm.

reveals sympathetic neurons (An et al., 2002). Frozen sections (15 μm) of embryos were collected on gelatin-coated slides, blocked in 0.5 M NaCl, 0.01 M phosphate buffer (PBS) (pH 7.0) with 5% normal goat serum and 0.1% Triton X-100 (block solution), incubated with polyclonal anti-tyrosine hydroxylase (Pel-Freez Biologicals, Brown Deer, Wisconsin) at 1:100 dilution in block solution, rinsed extensively in PBS with 0.1% Triton X-100, incubated in commercially available rhodamine-labeled goat anti-rabbit IgG secondary antibody (Jackson ImmunoResearch, West Grove, PA) diluted in block solution, and rinsed again. Embryos were examined on a Leica DMRA2 compound microscope and photographed with a Q-imaging Retiga 1300 digital camera and Open-

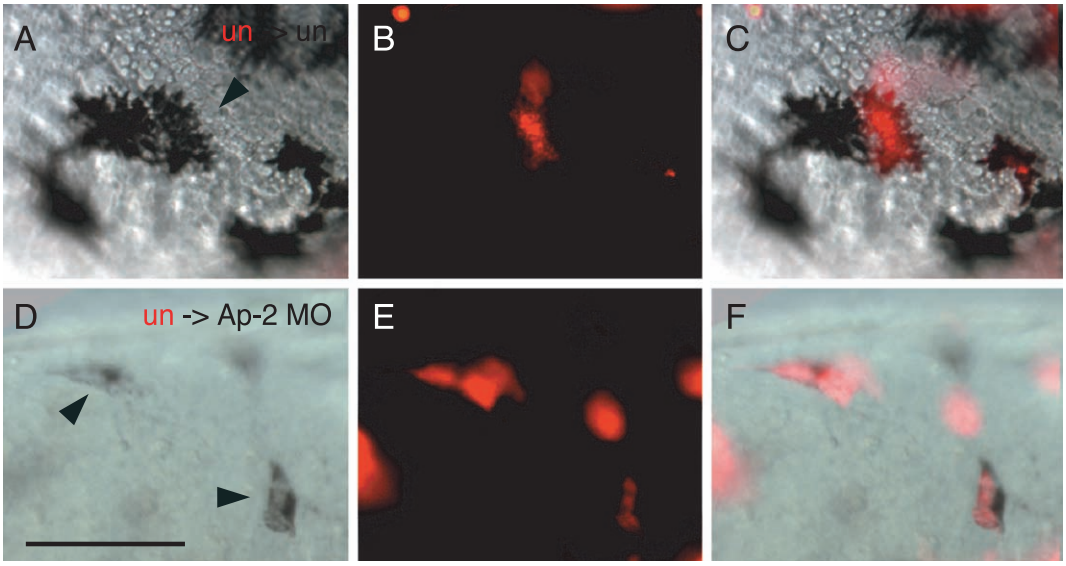

Fig. 5. Analysis of cell autonomy of melanophore differentiation phenotype. Close-up views of melanophores in 30-hpf embryos.(A and D) bright field, (B and E) fluorescent view, (C and F) merged view. (A–C) A labeled melanophore derived from a cell transplanted from a control donor into a control host (arrowhead). The labeled melanophore was similar in size, number of dendrites, and density of pigmentation as the adjacent host-derived melanophore (60 control-to-control transplants scored, three or more labeled melanophores observed in 14 embryos). (D–F) Labeled melanophores, derived from a control donor, in an *ap-2α* MO host (arrowheads). The melanophore was similar in shape and color to host-derived melanophores, but smaller, less dendritic, and under-pigmented in comparison to labeled melanophores in equivalently staged control-to-control transplants (50 control-to-*ap-2α* MO transplants scored, three or more labeled melanophores observed in 12 embryos). In converse experiment, 200 *ap-2α* MO-to-control transplants were scored, 95 embryos with labeled cells in neural tube were closely examined, but labeled melanophores were detected in none.

Table 1
Reduction in total number and migration of trunk melanophores in wild-type and *c-kit* heterozygous mutant embryos at 42 hpf after injection of *ap-2α* morpholino

Dose of E2I2 MO	Trunk melanophores			
	Wild type		*c-kit*$^{+/-}$	
	Total[a]	Ventral (%)[b]	Total	Ventral (%)
uninjected	69.1 ± 8.1	43.5 ± 3.4	71.0 ± 5.7	43.5 ± 2.9
0.2 mg/ml	60.8 ± 5.5	41.3 ± 5.3	49.4 ± 7.5*	24.5 ± 10.1*
0.4 mg/ml	52.2 ± 6.1	35.1 ± 6.6	42.1 ± 8.6**	17.7 ± 11.4*
0.8 mg/ml	47.4 ± 8.4	30.1 ± 6.4	34.2 ± 5.6**	14.0 ± 8.6*

[a] Total number of melanophores in dorsal, lateral and ventral stripes, counted in the eight somite region of trunk rostral to the anus. $n = 10$ for all treatments.
[b] Percentage of total melanophores in ventral stripe.
* Significantly different from wild-type at same dose, $P < 0.001$ (Student's t test).
** Significantly different from wild-type at same dose, $P < 0.005$ (Student's t test).

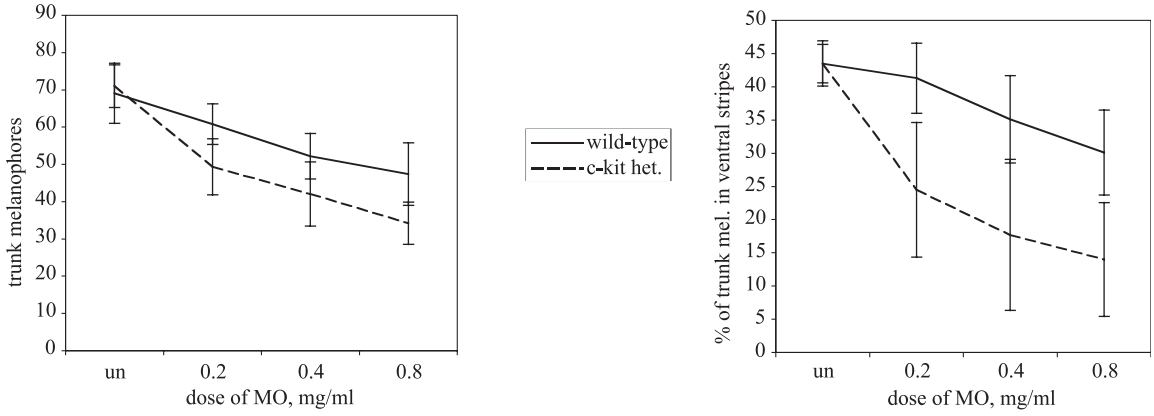

lab 3.1.2 software, and figures were assembled, and brightness and contrast manipulated, in Photoshop 7.0.

Transplants

Two to five nanoliters of 1% rhodamine-labeled dextran (10 000 mw, Molecular Probes) was injected into the yolk cell of donor embryos and 2–5 nl of 0.9 mg/ml unlabeled *ap-2* E2I2 morpholino was injected into the yolk cell of host embryos at the 2–4 cell stage. Alternatively, 2–5 nl of 0.9 mg/ml rhodamine-labeled *ap-2* E2I2 morpholino was injected into donor embryos, and hosts were uninjected (while the labeled morpholino was sufficiently bright to serve as lineage tracer for donor-derived cells, in some experiments, rhodamine-labeled dextran was added to the morpholino to increase brightness further). At the 1000 cell stage, 20–50 cells were removed from donor embryos by gentle suction and deposited near the margin of hosts of the same stage. Embryos were raised to 30 hpf. Using a stereomicroscope mounted with fluorescence optics, embryos with labeled cells in the neural tube were identified (approximately 50% of surviving transplants, regardless of whether donor or host was injected with morpholino). Such embryos were examined for labeled melanophores on a compound fluorescence microscope. At 30 hpf, morpholino-injected embryos were approximately 2 h delayed in development with respect to control embryos. Comparison of melanophore morphology was performed between equivalently staged embryos.

Results

Zebrafish ap-2α is expressed in premigratory neural crest

The two zebrafish variants of *ap-2* cDNA isolated by Furthauer et al. (1997) most closely resemble mammalian *Ap-2α* (84.7% identical to human AP-2α, Williams et al., 1988; 68.1% identical to human AP-2β, Moser et al., 1995; and 59.9% identical to human AP-2γ; McPherson et al., 1997), so we refer to them as *ap-2α* isoforms 1 and 2. The isoforms differ from one another only at their 5′ ends, and analysis of genomic sequence revealed the alternate leader sequences are present as single exons upstream of the shared exons (see Methods). The leader sequences are homologous to those of two mouse isoforms of *Ap-2α* (Fig. 1), suggesting there may be functional significance to them. In mouse embryos, several of first-exon isoforms of *AP-2α* are expressed in overlapping but distinct domains (Meier et al., 1995; Mitchell et al., 1991). The zebrafish isoforms differ by less than 100 bp, and our attempts to resolve their

individual expression patterns by whole mount in situ hybridization were unsuccessful.

Whole mount in situ hybridization of neurula stage embryos, using a probe that hybridizes to both isoforms of *ap-2α*, revealed that at 12 hpf, *ap-2α* was expressed in premigratory neural crest (PNC) of the lateral neural plate and in presumptive epidermis but excluded from rest of the neural plate, as previously reported (Furthauer et al., 1997). Double in situ analysis with an early marker of premigratory neural crest, *foxd3*, confirmed that these genes are expressed in the same cells, and showed that *ap-2α* expression slightly precedes *foxd3* expression in this region (Fig. 1). At 17 hpf, expression was detected in migrating cranial neural crest (Fig. 1E) and trunk dorsal neural tube (Fig. 1F). By 24 hpf, expression was detected in lateral line primordium (Fig. 1G), perhaps in Schwann cells associated with it, but not near melanoblasts or elsewhere on trunk neural crest migratory pathways. These results suggest *ap-2α* is expressed in premigratory trunk neural but extinguished shortly after these cells delaminate from the dorsal neural tube. It is not clear when cells of vagal neural crest, whose migratory pathway has not been well characterized, lose expression of *ap-2α*.

Antisense morpholinos disrupt splicing of ap-2α transcripts

In zebrafish embryos, injection of morpholinos that are complementary to exon boundaries can direct splice machinery to choose alternate splice donor sites (Draper et al., 2001). To target all first-exon variants of *ap-2α*, morpholinos were designed to complement the exon 2–intron 2 (E2I2 MO) or the exon 3–intron 3 (E3I3 MO) splice donor sites. The effect of these MO on splicing of the *ap-2α* transcripts was tested by isolating RNA from uninjected control or morpholino-injected embryos, synthesizing first-strand cDNA, and amplifying *ap-2α* cDNAs (RT-PCR analysis) (Fig. 2). Both morpholinos caused mis-splicing of a fraction of *ap-2α* RNA, resulting in internal deletions of these transcripts that would be expected to prevent function of the encoded proteins (Fig. 1; Wankhade et al., 2000). Embryos injected with E2I2 MO, referred to below as *ap-2α* MO embryos, were analyzed for defects in neural crest derivatives. Specificity of each phenotype was subsequently confirmed by analysis of embryos injected with E3I3 MO, or with negative-control morpholinos (see Methods).

Neural-crest-derived melanophores are reduced in ap-2α MO embryos

In *ap-2α* MO embryos, there were no gross abnormalities of gastrulation and early morphogenesis, in contrast to mice homozygous for targeted mutation of *Ap-2α* (Schorle et al., 1996; Zhang et al., 1996), and frog embryos injected with *ap-2*-function-blocking oligonucleotides (Luo et al., 2002). The first visible phenotypes in zebrafish *ap-2α* MO embryos were within neural crest-derived melanophores, which had multiple defects. At 28 hpf, when black, dendritic melanophores were visible in the heads of uninjected embryos (Fig. 3A), in *ap-2α* MO embryos, melanophores were pale and small (Fig. 3B). By contrast, eye pigmentation was normal at this and later stages. At 42 hpf, only about 40% of the normal number of melanophores were present in *ap-2α* MO embryos (Figs. 4A and B). Moreover, the fraction of trunk melanophores present in ventral stripes (contacting the hindyolk) was also reduced in *ap-2α* MO embryos (Figs. 4A and B, Table 1), implying Ap-2α function is required for normal melanophore migration. At 48 hpf, the morphology and color (but not number) of melanophores had largely recovered in *ap-2α* MO embryos. It is unclear whether melanophores recover because they become independent of Ap-2α function at this stage, or because of diminishing efficacy of morpholinos. No defects on xanthophores and on iridophores were detected in *ap-2α* MO embryos.

Expression of pigment cell markers was examined in *ap-2α* MO embryos. *mitf*, a gene required for specification of melanoblasts (*nacre* mutant, Lister et al., 1999), was expressed in fewer cells than normal at 24 hpf (Figs. 3C and D), although the level of expression of this gene within single cells appeared normal, suggesting *mitf* is not directly regulated by Ap-2α. In contrast, *dopachrome tautomerase* (*dct*), which encodes a tyrosinase family member necessary for melanin synthesis (Pawelek and Chakraborty, 1998), was expressed at much lower levels within individual cells in 24 hpf *ap-2α* MO embryos (Figs. 3E and F). A reduction of Dct may explain why melanophores are underpigmented at 28 hpf. Similarly, *c-kit*, which encodes a receptor tyrosine kinase implicated in regulation of proliferation and survival of melanophores (Parichy et al., 1999), was expressed in fewer neural crest cells and at lower levels in 24 hpf *ap-2α* MO embryos than in uninjected embryos (Figs. 3G and H). By contrast, expression of *c-kit* in cells near the anus was unchanged in *ap-2α* MO embryos, revealing distinct regulation of *c-kit* expression in that tissue (Figs. 3G and H). Finally, expression of *ednrb1,* which encodes a putative receptor for endothelin-3 and is essential for adult but not embryonic melanoblasts (Parichy et al., 2000a), was similar to *mitf* in that it was expressed at normal levels, but in fewer cells than normal (not shown). Expression of *c-fms*, a *c-kit* homolouge expressed in xanthophore precursors (Parichy et al., 2000b), appeared normal in *ap-2α* MO embryos (not shown).

Genetic interaction between Ap-2α and C-kit

The reduction of *c-kit* expression in *ap-2α* MO embryos suggests that Ap-2α and C-kit function in the same pathway to regulate melanophore cell number and migration. Consistent with this notion, *c-kit* heterozygotes injected with sub-maximal doses of *ap-2α* morpholino had fewer melanophores than similarly injected wild-type embryos (Table

1). To test whether Ap-2α regulates melanophore number and migration entirely via the activation of *c-kit,* embryos homozygous for a null allele of *c-kit* were injected with *ap-2α* E2I2 morpholino. At 40 hpf, *ap-2α* MO-injected *c-kit* mutant embryos had fewer melanophores overall, and a lower percentage in ventral positions, than uninjected *c-kit* mutant embryos (Figs. 4C and D). This implies the existence of at least one additional target of Ap-2α regulating melanophore cell number and migration.

Control of melanophore development by Ap-2α is both cell autonomous and non-autonomous

Because *ap-2α* is expressed in neural crest and encodes a transcription factor likely to bind the *c-kit* promoter, its function is presumably at least partially cell autonomous to melanophores. However, *ap-2α* is also expressed in the presumptive epidermis, so potentially, Ap-2α could regulate the expression of a gene in the skin that would influence melanophore development in a cell-non-autonomous fashion. To test these possibilities, mosaic embryos were created by transplanting cells at blastula stage between control embryos and *ap-2α* MO embryos. Melanophores that derived from control cells transplanted into control hosts appeared normal, and were indistinguishable in color and shape from host-derived melanophores (Figs. 5A–C). Unexpectedly, we observed that melanophores derived from control cells transplanted into *ap-2α* MO host embryos were underpigmented and non-dendritic, just as were host-derived, morpholino-containing melanophores (Figs. 5D–F). If the activity of Ap-2α was entirely cell autonomous to melanophores, melanophores deriving from control cells should have been clearly distinct in size and color from host-derived melanophores in *ap-2α* MO embryos. This implies that Ap-2α has a cell-non-autonomous role in regulation of melanophore differentiation. In the converse experiment, melanophores that derived from *ap-2α* MO cells transplanted into control embryos were never detected (Fig. 5C), despite analysis of more than 100 such transplants. These results suggest that Ap-2α has both cell-autonomous and cell-non-autonomous roles in regulation of melanophore size and color.

Multiple neural crest derivatives were reduced in ap-2α MO embryos

Because Ap-2α is required for normal jaw patterning in mouse embryos (Schorle et al., 1996; Zhang et al., 1996), pharyngeal cartilage was examined in *ap-2α* MO embryos at 4 dpf. Characteristic cartilage defects were observed, most clearly in the bilateral ventral elements of pharyngeal arch two (p2), the cerratohyals (Fig. 6). In *ap-2α* MO embryos, the cerratohyals were reduced in size and pointed medially (instead of rostrally) (Fig. 6). More posterior arches (p3–p7; cerratobranchials) were less affected but were variably reduced in size in strongly affected *ap − 2α* MO embryos (about 10% of embryos injected with either E2I2 or E3I3 morpholino). In contrast, Meckel's cartilage and the palatoquadrate, first-arch (p1) derivatives, were relatively normal in size; however, in strongly affected embryos they pointed ventrally (Fig. 6).

Some neuronal derivatives of neural crest were affected in *ap-2α* MO embryos. Ap-2α directly binds and activates the tyrosine hydroxlase and dopamine β-hydroxylase (*DBH*) promoters (Greco et al., 1995; Kim et al., 2001). In *ap-2α* MO embryos, the number of cells expressing tyrosine hydroxylase near the dorsal aorta at 4 dpf, indicative of neural crest-derived sympathetic neurons and adrenal chromaffin cells (An et al., 2002), was highly reduced (Fig. 6). Dorsal root ganglion neurons appeared normal in *ap-2α* MO embryos, similar to mouse Ap-2α mutants (Schorle et al., 1996; Zhang et al., 1996). Interestingly, enteric neurons, which are derived from vagal neural crest (Le Douarin and Kalcheim, 1999), were dramatically reduced in *ap-2α* MO embryos (Fig. 6). In contrast to mouse Ap-2α mutants, markers of trigeminal ganglia (Zn 12 immunoreactivity at 30 hpf, anti-Hu immunoreactivity at 4 dpf) (results not shown, see Methods) were not dramatically changed in *ap-2α* MO embryos.

Fig. 6. Zebrafish *ap-2α* MO embryos have reduced neural crest derivatives. Lateral (A and B) and ventral (C and D) views of 4-dpf embryos processed to reveal craniofacial cartilage. (A and C) Uninjected embryo and (B and D) *ap-2α* MO embryo. In injected embryos, 41 of 110 exhibited characteristic abnormal craniofacial architecture. Hyosymplectic (hs) and ceratohyal (ch) are dorsal and ventral elements of the p2, respectively (see Schilling et al., 1996). In *ap-2α* MO embryos, the ceratohyals were reduced in size and abnormally shaped. The hyosymplectics were present but not as extended as in wild-type embryos. The cerratobranchials, derived from p3–p7, were variably reduced in strongly affected embryos. p1 derivatives, Meckel's cartilage (m) and palatoquadrate (pq), appeared somewhat reduced in size and in strongly affected embryos (10/110 embryos injected with E2I2 MO), pointed ventrally. These phenotypes are highly reminiscent of the *lockjaw* mutant phenotype (Schilling et al., 1996), except less severe. For instance, in *lockjaw* mutant embryos, ceratobranchial elements are absent, but they are merely smaller in *ap-2α* MO embryos. The milder phenotype of *ap-2α* MO embryos suggests Ap-2α function is reduced but not eliminated in them. (E and F) Lateral view of embryos fixed at 4 dpf and processed to reveal anti-Hu-immunoreactivity. (E) In uninjected embryos, enteric neurons (e) dorsal root ganglion (drg) neurons are revealed by anti-Hu immunoreactivity. (F) In *ap-2α* MO embryos, enteric neurons (e) were highly reduced (anti-Hu+ enteric neurons in the section of gut overlying the hindyolk: uninjected embryos, 99.2 ± 13.2, *ap-2α* MO embryos, 22.2 ± 10.1, $n = 6$, $P < 0.0001$, Student's *t* test). (G and H) Transverse sections, near axial level of pectoral fins, of 4-dpf embryos processed to reveal anti-tyrosine hydroxylase immunoreactivity (TH-IR). (G) In uninjected embryos, TH-IR ventral to notochord (n) is in sympathetic neurons, while TH-IR in more ventral and lateral position is in adrenal chromaffin cells (An et al., 2002) (arrowheads; average of 36 ± 5 sympathetic neurons, $n = 5$ embryos.) (H) In *ap − 2α MO* embryos, there was a significant reduction of TH-IR positive cells (average of 7 ± 1 TH-IR positive cells in *ap-2α* MO embryos that showed reduced numbers of melanophores at 30 hpf, $n = 5$, $P < 0.005$). All scale bars, 100 μm. Scale bar in B applies for both A and B, etc.

In mice, neural crest cells contribute to cardiac outflow tract development, and Ap-2α is required for outflow tract morphogenesis (Brewer et al., 2002). Recent studies in zebrafish have suggested that some cranial neural crest cells contribute to cardiac muscle and that ablation of neural crest cells leads to decreased contractility and aberrant cardiac morphology by 2 dpf (Li et al., 2003). However, in *ap-2α* MO embryos at 2 dpf, blood flow,

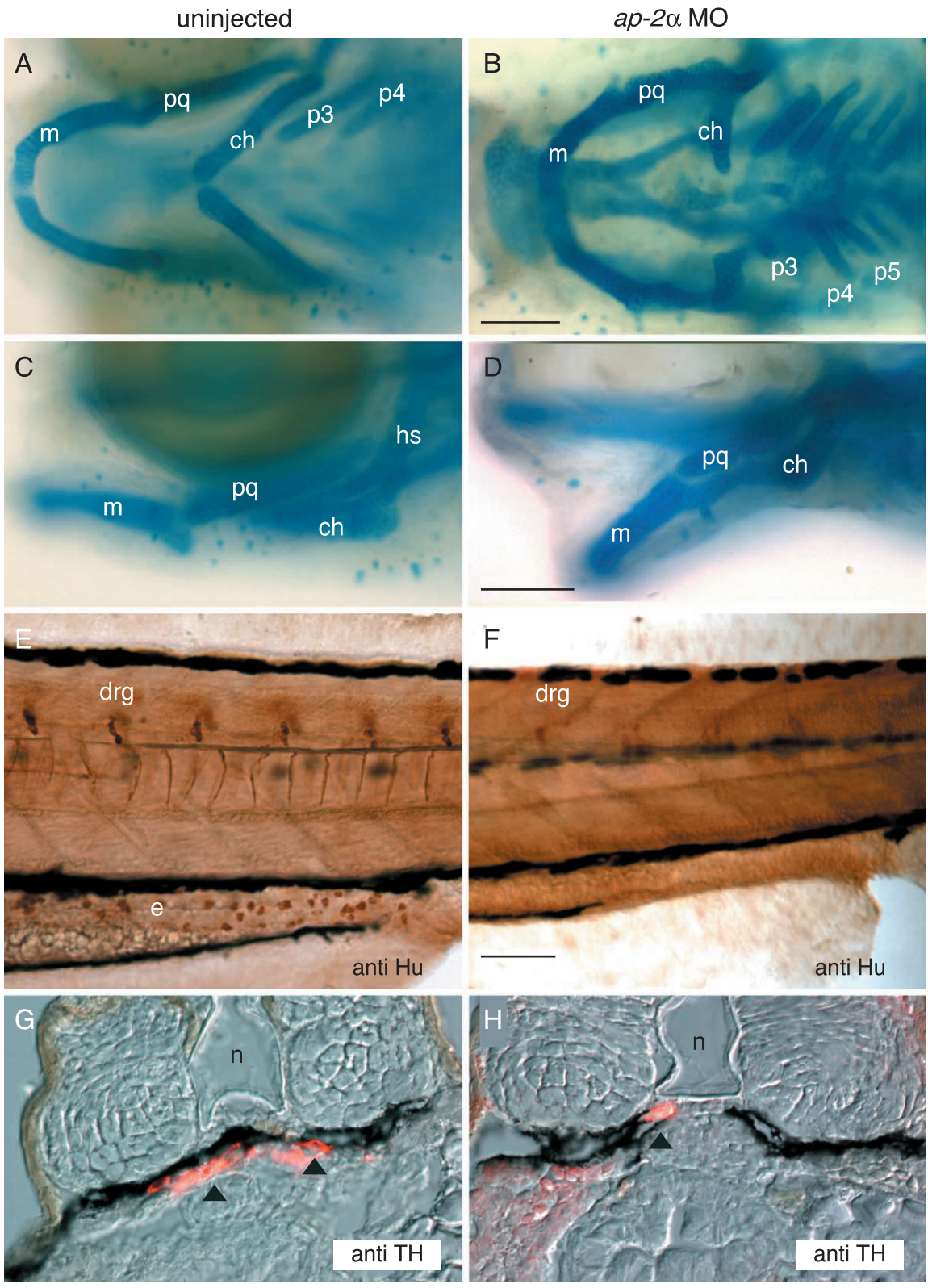

cardiac morphology, and heart rate were all normal (99 ± 7 bpm in controls, 97 ± 6 bpm in *ap-2α* MO embryos, $n = 10$, Student's t test, $P = 0.4$). Starting at 3 dpf, *ap-2α* MO embryos exhibited pericardial edema (results not shown), as is typically found in zebrafish embryos with cardiovascular insufficiency. However, it is unclear whether edema arising at this stage results from a direct influence of Ap-2α on the heart or as a secondary consequence of abnormal aortic arch formation (Isogai et al., 2001) (e.g. p3 in Fig. 6B).

ap-2α MO embryos have reduced expression of cranial neural crest markers

Because multiple neural crest derivatives were abnormal in *ap-2α* MO embryos, a primary defect in neural crest was indicated. In addition, *ap-2α* is expressed in zebrafish neural crest (Furthauer et al., 1997; Nguyen et al., 1998), and inhibition of AP-2 in frog blocks expression of markers of premigratory neural crest (Luo et al., 2003). In contrast, in *ap-2α* MO embryos at 11 hpf, expression of two markers of

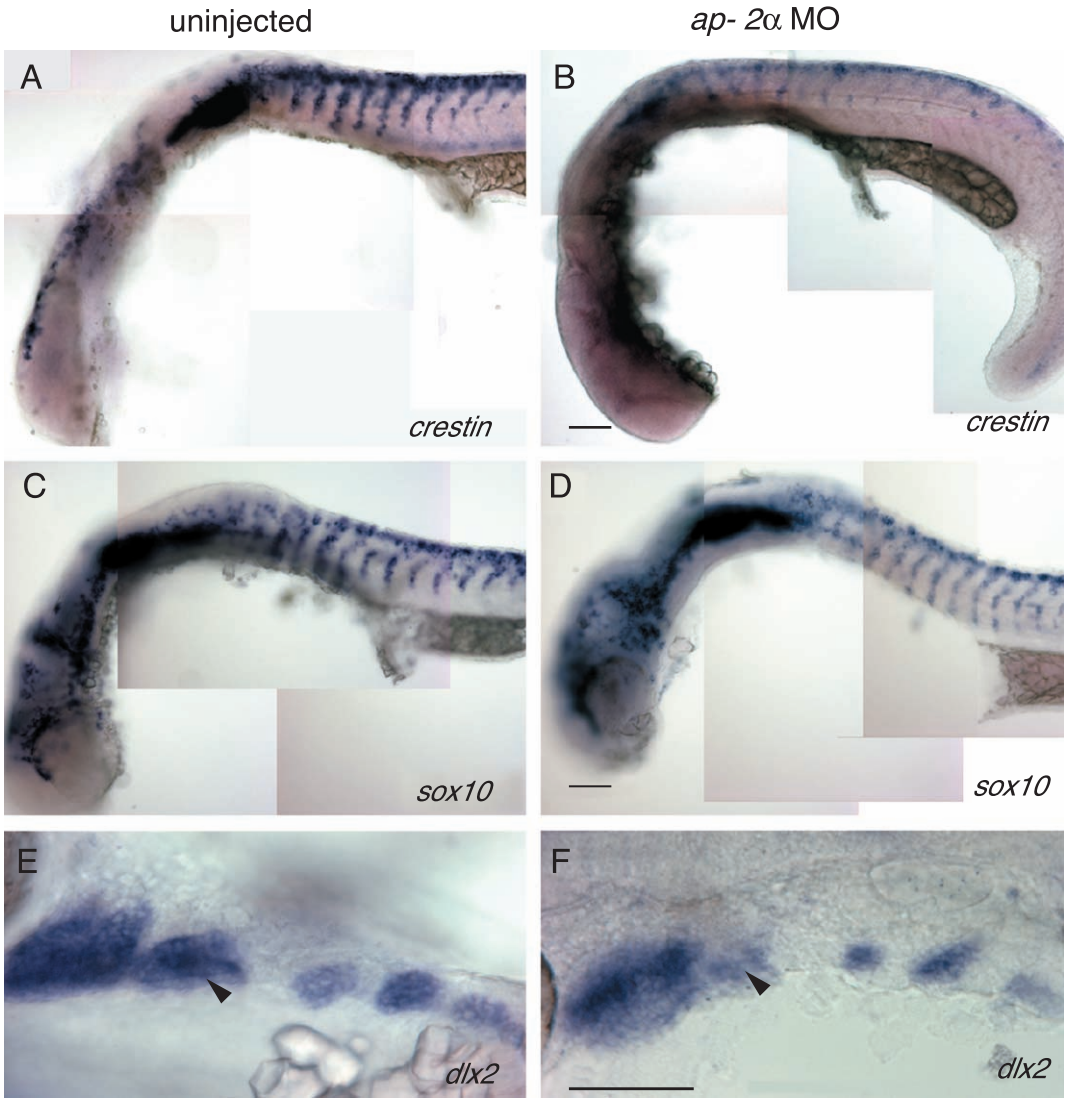

Fig. 7. Zebrafish *ap-2α* MO embryos have reduced cranial neural crest cells. Lateral view of 24-hpf (A) uninjected embryo and (B) *ap-2α* MO embryo processed to reveal *crestin* expression, a marker of migrating neural crest at this stage (Luo et al., 2001). The intensity of *crestin* expression was much lower in individual cells of *ap-2α* MO embryos, and the number of *crestin*-expressing cells appeared to be reduced. (C and D) Lateral view of 20-hpf (C) uninjected embryo or (D) *ap-2α* MO embryo processed to reveal *sox10* expression. Expression was normal, or very slightly reduced as in the embryo pictured here, in *ap-2α* MO embryos. (E and F) Lateral view of 24-hpf (E) uninjected embryo and (F) a strongly affected *ap-2α* MO embryo, processed to reveal *dlx2* expression, a marker of neural crest migrating in pharyngeal arches at this stage (Akimenko et al., 1994). Relative to uninjected embryos, in a majority of *ap-2α* MO embryos, a clear reduction of *dlx2*-expressing cells was seen in p2 (arrowhead), and in strongly affected *ap-2α* MO embryos, a reduction of *dlx2*-expressing cells was also apparent in more caudal arches (8/90 embryos scored). The number of *dlx2*-expressing cells in p1 appeared normal in *ap-2α* MO embryos. All scale bars, 100 μm. Scale bar in B applies for both A and B, etc.

premigratory neural crest, *foxd3* and *sox10,* was normal (results not shown; Dutton et al., 2001b; Odenthal and Nusslein-Volhard, 1998). In *ap-2α* MO embryos at 20 and 24 hpf, expression of *sox10* in migrating neural crest marker appeared normal, although we note that this gene is not a marker of migrating neural crest in pharyngeal arches (Fig. 5 and not shown, Dutton et al., 2001a). Surprisingly, in contrast to *sox10*, expression of *crestin* was globally reduced at 24 hpf (Luo et al., 2001; Rubinstein et al., 2000). At 24 hpf in *ap-2α* MO embryos, abnormal expression of *dlx2*, a marker of cranial neural crest in pharyngeal arches (Akimenko et al., 1994), was detected. In majority of *ap-2α* MO embryos, fewer cells of pharyngeal arch 2 (p2) expressed *dlx2*, and in strongly affected embryos, expression was also reduced in p2−p7 (Fig. 7). Expression of *dlx2* in p1 was relatively unaffected in all *ap-2α* MO embryos (Fig. 7 and not shown). Thus, migrating neural crest is present in *ap-2α* MO embryos, although its gene expression profile is abnormal and neural crest in p2−p7 may be reduced.

Discussion

ap-2α MO embryos complete early development normally

Even at maximal doses, morpholinos targeting *ap-2α* did not cause the gross defects in morphogenesis seen in mouse *Ap-2α* mutants, which include failure of closure of cranial neural folds, or closure of the ventral body walls in mouse embryos (Schorle et al., 1996; Zhang et al., 1996). Moreover, in frog embryos injected with *AP-2* antisense oligonucleotides, there is an apparent absence of neural crest and a cessation of development shortly after gastrulation (Luo et al., 2003). In zebrafish, *ap-2α* MO embryos migratory neural crest is clearly present, although its gene expression profile is altered, and cranial neural crest cells in P2−P7 may be reduced, as expression of *dlx2* is seen in fewer cells there. In zebrafish *ap-2α* MO embryos, early roles for AP-2α in morphogenesis and neural crest formation may be performed by residual Ap-2α protein. Indeed, full-length *ap-2α* transcripts that escaped the morpholino were always detected in RT-PCR experiments carried out on *ap-2α* MO embryos. Alternatively, additional Ap-2α homologues may function in early zebrafish development; a recent search of public sequence data revealed the presence of at least three additional *ap-2α* homologues in the zebrafish genome (W.L. and R.A.C., unpublished observations, Sanger Consortium). Misexpression of dominant negative Ap-2α proteins may be a more effective way to block all Ap-2α function (see Buettner et al., 1993). Whatever the explanation for their normal early development, *ap-2α* MO embryos are well suited for analysis of Ap-2α function in neural crest derivatives, particularly in derivatives that arise after the time of death of mouse *Ap-2α* mutant embryos.

Ap-2α regulates melanophore development via C-kit and other targets

Melanophore defects in *ap-2α* MO embryos make sense in light of the suspected regulation of *C-KIT* by Ap-2α in human cells. *C-kit* encodes a receptor for the ligand Steel and is required for proliferation, survival, and perhaps differentiation of melanoblasts in mice (Ito et al., 1999; Kunisada et al., 1998; Steel et al., 1992). In zebrafish *c-kit* null mutants (i.e., *sparse*), melanophores are reduced in number and cluster near the dorsal neural tube (Parichy et al., 1999). In *ap-2α* MO embryos, *c-kit* expression is reduced, trunk melanophores are reduced in number and in extent of migration. Importantly, our observation that a given dose of *ap-2α* morpholino has a greater effect on melanophore cell number and migration in *c-kit* heterozygotes than in wild types is strong evidence that these two genes work in the same pathway in melanophores. The regulation of *c-kit* by Ap-2α is likely direct: the human *C-KIT* promoter contains AP-2 consensus binding sites, and overexpression of *AP-2α* in melanoma cell lines increases *C-KIT* expression (Huang et al., 1998). However, Ap-2α appears to regulate melanophore number and migration via additional targets because injection of the *ap-2α* morpholino further reduces melanophores in *c-kit* homozygous null mutant embryos. Moreover, in *ap-2α* MO embryos at 28 hpf, melanophores are not as black as usual, indicating reduced melanin synthesis, and they appear smaller and less dendritic than normal. While activation of the C-kit pathway can stimulate differentiation of mouse melanoblasts (Kunisada et al., 1998), abnormal melanophore differentiation is not seen in zebrafish *c-kit* mutant embryos (Parichy et al., 1999), again suggesting other or additional effectors of melanophore differentiation by Ap-2α.

What other targets of Ap-2α regulate melanophores? Candidates include other *c-kit* orthologues, although *c-fms*, a *c-kit* homologue required by embryonic xanthophores, was normal in *ap-2α* MO embryos, showing that not all *c-kit* homologues depend on Ap-2α. A reduction of melanin is consistent with reduced levels of *dct* expression in *ap-2α* MO embryos. The regulation of *dct* may be mediated by Melanocyte-Specific Gene 1 (MSG1), which contains potential binding sites for Ap-2α in its promoter (Fenner et al., 1998) and which upon overexpression in melanoma cells leads to expression of *tyrosinase* and *dopachrome-tautomerase* (*DCT*), and increased melanin (Nair et al., 2001). Other potential Ap-2α targets include components of the pathway stimulated by the Endothelin receptor type b (Ednrb). As in *ap-2α* MO embryos, mouse embryos homozygous for a targeted deletion of *Ednrb* have reduced numbers of melanocytes (Hosoda et al., 1994; Lee et al., 2003; Shin et al., 1999) and Ednrb signaling stimulates proliferation and perhaps differentiation of mammalian melanoblasts (Lahav et al., 1996). Furthermore, Ednrb function is also known to be required for correct migration of enteric neurons (Lee et al., 2003). Finally, both Ap-2α

and Ednrb appear to repress differentiation of Schwann cells (Brennan et al., 2000; Stewart et al., 2001). In zebrafish, only one *ednrb* orthologue has been described to date, and it is expressed in embryonic melanoblasts. Mutations in this gene lead to a reduction of adult melanophores, however, embryonic melanophores and enteric neurons appear normal (Parichy et al., 2000a). Therefore, it is most likely that a separate Ednrb orthologue functions in these cell types. Nonetheless, the observation that melanoblast expression of *ednrb1* is normal in residual melanoblasts in *ap-2α* MO embryos suggests that any interaction between Ednrb and Ap-2α pathways is not at the level of receptor expression. Because the role of Ap-2α is partially cell non-autonomous, one possibility is that Ap-2α regulates expression of the ligand endothelin-3.

Cell autonomy of Ap-2α function in melanophores

A cell-non-autonomous role for Ap-2 in melanophore development was unexpected, but is consistent with essential roles for Ap-2 homologues in epidermal development. Thus, melanophores derived from control cells transplanted into *ap-2α* MO embryos did not have a wild-type appearance, but instead were small and underpigmented. This result could not be explained by a global delay of development caused by the morpholino, because the phenotype of small, pale melanophores was observed in closely stage-matched embryos, as judged by the development of the eye and progression of the lateral line primordium. This result implies that Ap-2α function is required in another tissue in addition to melanophores to support their normal differentiation. Melanophores are closely apposed to skin. In *X. laevis*, reduction of AP-2 function appears to cause epidermal precursors to adopt a neural fate, implying a very early role for AP-2 in specification or maintenance of the epidermal fate (Luo et al., 2002). In human skin, nuclear expression of Ap-2α is highest in the basal layer of keratinocytes, suggesting it regulates their proliferation, or perhaps limit their differentiation (Mazina et al., 2001; Oyama et al., 2002). Ap-2γ is expressed in all layers of epidermal cells, and may also be important for keratinocyte differentiation (Oyama et al., 2002). It will be important to assess epidermal development in *ap-2α* MO embryos to address this hypothesis.

Ap-2α is also expected to be required within melanoblasts, for instance to activate the *c-kit* promoter. However, it is unclear why we were unable to detect labeled melanophores in *ap-2α* MO-to-control transplants, despite scoring enough such transplants that we predicted seeing them in about 30 embryos. Perhaps the melanophores containing the *ap-2α* MO were delayed or hidden by the large, black melanophores of the host. An intriguing alternative explanation is that neural crest cells or melanoblasts inheriting *ap-2α* MO succumb to death signals, or signals that induce them to adopt a different fate, which are present in control hosts but are reduced in an *ap-2α* MO hosts.

Other neural crest derivatives depend on Ap-2α

Defects in several other neural crest derivatives were detected in *ap-2α* MO embryos, suggesting zebrafish may be a useful model for analysis of neurocristopathies. *ap-2α* MO embryos like mouse *Ap-2α* mutants have an abnormal pharyngeal skeleton. Elements of p2 were most sensitive to the *ap-2α* morpholino, with more caudal arches reduced in strongly affected embryos, implying a quantitative difference in dependence on Ap-2α function in these structures. Derivatives of p1, Meckel's cartilage and the palatoquadrate, were relatively normal in *ap-2α* MO embryos (Fig. 6). These elements were also normally patterned, although slightly reduced in size, in homozygous *lockjaw* mutant embryos, which harbor null alleles of *ap-2α* (Schilling et al., 1996; T. Schilling, personal communication). Thus, Ap-2α function may be limited to neural crest contributing to p2 and more posterior arches. Consistent with this model, in mouse embryos, p2 is the anterior limit of *hoxa2* expression, a gene that is activated by Ap-2α (Hunter and Prince, 2002; Maconochie et al., 1999). Indeed, the role of Ap-2α in p2 elements may be largely or entirely mediated by its effect on *hox* paralogue group 2 genes (*hoxa2* and *hoxb2*), because p2 elements are abnormal in embryos in which these genes have been inhibited with morpholinos (hox pg2 morphants, see Hunter and Prince, 2002). Ap-2α may also interact with more posteriorly expressed Hox genes, because p3–p7 derivatives, which are relatively normal in *hox pg2* MO embryos, are clearly abnormal in severely affected *ap-2α* MO embryos and *lockjaw* mutant embryos. Because the hyoid arch was the most affected in *ap-2α* MO embryos, it is notable in the mouse *Ap-2α* mutant, the hyoid, which derives from pharyngeal arches 2 and 3, was reported to be normal in mouse mutants (Zhang et al., 1996). The mouse phenotype was reported to include an absence of the stapes bone (p2 derived) but the presence of the mandible (p1 derived) (Schorle et al., 1996; Zhang et al., 1996). It is unclear in mouse *Ap-2α* mutants whether defects in pharyngeal skeleton reflect a direct dependence of cranial neural crest on Ap-2α, or whether they are secondary to defects in closure of cranial neural folds (Schorle et al., 1996; Zhang et al., 1996). In zebrafish *ap-2α* MO embryos, changes in *dlx2* expression predicted the changes in pharyngeal skeleton, implying a direct role for Ap-2α in neural crest patterning. These results are interesting because human *Ap-2α* is located on chromosome 6p24, a region that has been linked to nonsyndromic cleft lip and palate in many studies (Carinci et al., 1995; Prescott et al., 2000; Scapoli et al., 1997).

Analysis of *ap-2α* MO embryos revealed a requirement for Ap-2α function in autonomic neurons of sympathetic and enteric ganglia. Most of the sympathetic ganglion chain derives from trunk neural crest, but the first detectable sympathetic neurons in zebrafish are rostral ones that likely originate in vagal (hindbrain) neural crest (An et al., 2002). These cells express Tyrosine Hyrdoxylase (TH), an enzyme required for synthesis of catecholamines. Anti-TH immu-

noreactivity was reduced in the normal vicinity of sympathetic neurons in *ap-2α* MO embryos. Ap-2α has been shown to directly bind the regulatory regions of genes encoding TH and dopamine β-hydroxylase, another enzyme involved in the biosynthesis of catecholamines (Greco et al., 1995; Kim et al., 2001, 1998; Yang et al., 1998). In addition, *ErbB2*, which encodes a receptor for the growth factor Neuregulin-1, is activated by Ap-2α (Bosher et al., 1995), and *ErbB2* mutants suffer severe hypoplasia of the sympathetic ganglion chain, apparently from a failure of neural crest migration (Britsch et al., 1998). These observations suggest Ap-2α regulates the multiple steps of sympathetic neuron development. In addition, enteric neurons, which also derive from vagal neural crest, were virtually eliminated from the hindgut of strongly affected *ap-2α* MO embryos. It is unclear what step in the development of enteric neurons (i.e., specification, differentiation, survival, or migration) depends on Ap-2α. This result was not anticipated by previous work, but is of interest in light of congenital defects of the enteric nervous system, such as Hirschsprung's disease, a multifactorial disorder characterized by aganglionic colon (OMIM 142623, reviewed in Passarge, 2002) or Waardenburg–Shah syndrome, characterized by pigment and enteric ganglia abnormalities (OMIM 277580, Shim et al., 1999). Indeed, it is possible that mutations in *AP-2α* confer susceptibility to these diseases.

In conclusion, because they complete early development relatively normally, analysis of zebrafish *ap-2α* MO embryos has revealed previously unrecognized roles for Ap-2α in neural crest patterning. The zebrafish model should be useful in the exploration of the roles the Ap-2α plays in normal development of neural crest derivatives, and possible roles for this protein in diseases that afflict neural crest derivatives, including malignant melanoma, Hirschsprung's disease, and cleft lip and palate.

Acknowledgments

We are grateful to Tom Schilling for sharing data before publication. We appreciate excellent technical assistance from Saxon McCloud and Jennifer Paulson, and the gift of *sparse* homozygotes from Stephen Johnson. This work was supported by NIH grant HD22486 to J.S.E. and a Carver Foundation seed grant to R.A.C. C. d'., and M.A. were supported by grants ICM P99-137-f and Fondecyt 1031003. E.K.O. was supported by Grant T32 DC00040 (Bruce Gantz, PI).

References

Akimenko, M.A., Ekker, M., Wegner, J., Lin, W., Westerfield, M., 1994. Combinatorial expression of three zebrafish genes related to distal-less: part of a homeobox gene code for the head. J. Neurosci. 14, 3475–3486.

An, M., Luo, R., Henion, P.D., 2002. Differentiation and maturation of zebrafish dorsal root and sympathetic ganglion neurons. J. Comp. Neurol. 446, 267–275.

Andermann, P., Ungos, J., Raible, D.W., 2002. Neurogenin1 defines zebrafish cranial sensory ganglia precursors. Dev. Biol. 251, 45–58.

Bauer, R., McGuffin, M.E., Mattox, W., Tainsky, M.A., 1998. Cloning and characterization of the *Drosophila* homologue of the AP-2 transcription factor. Oncogene 17, 1911–1922.

Baynash, A.G., Hosoda, K., Giaid, A., Richardson, J.A., Emoto, N., Hammer, R.E., Yanagisawa, M., 1994. Interaction of endothelin-3 with endothelin-B receptor is essential for development of epidermal melanocytes and enteric neurons. Cell 79, 1277–1285.

Bosher, J.M., Williams, T., Hurst, H.C., 1995. The developmentally regulated transcription factor AP-2 is involved in c-erbB-2 overexpression in human mammary carcinoma. Proc. Natl. Acad. Sci. U. S. A. 92, 744–747.

Brannan, C.I., Lyman, S.D., Williams, D.E., Eisenman, J., Anderson, D.M., Cosman, D., Bedell, M.A., Jenkins, N.A., Copeland, N.G., 1991. Steel-Dickie mutation encodes a c-kit ligand lacking transmembrane and cytoplasmic domains. Proc. Natl. Acad. Sci. U. S. A. 88, 4671–4674.

Brennan, A., Dean, C.H., Zhang, A.L., Cass, D.T., Mirsky, R., Jessen, K.R., 2000. Endothelins control the timing of Schwann cell generation in vitro and in vivo. Dev. Biol. 227, 545–557.

Brewer, S., Jiang, X., Donaldson, S., Williams, T., Sucov, H.M., 2002. Requirement for AP-2alpha in cardiac outflow tract morphogenesis. Mech. Dev. 110, 139–149.

Britsch, S., Li, L., Kirchhoff, S., Theuring, F., Brinkmann, V., Birchmeier, C., Riethmacher, D., 1998. The ErbB2 and ErbB3 receptors and their ligand, neuregulin-1, are essential for development of the sympathetic nervous system. Genes Dev. 12, 1825–1836.

Buettner, R., Kannan, P., Imhof, A., Bauer, R., Yim, S.O., Glockshuber, R., Van Dyke, M.W., Tainsky, M.A., 1993. An alternatively spliced mRNA from the AP-2 gene encodes a negative regulator of transcriptional activation by AP-2. Mol. Cell. Biol. 13, 4174–4185.

Carinci, F., Pezzetti, F., Scapoli, L., Padula, E., Baciliero, U., Curioni, C., Tognon, M., 1995. Nonsyndromic cleft lip and palate: evidence of linkage to a microsatellite marker on 6p23. Am. J. Hum. Genet 56, 337–339.

Chazaud, C., Oulad-Abdelghani, M., Bouillet, P., Decimo, D., Chambon, P., Dolle, P., 1996. AP-2.2, a novel gene related to AP-2, is expressed in the forebrain, limbs and face during mouse embryogenesis. Mech. Dev. 54, 83–94.

Cornell, R.A., Eisen, J.S., 2002. Delta/Notch signaling promotes formation of zebrafish neural crest by repressing Neurogenin 1 function. Development 129, 2639–2648.

Dorsky, R.I., Moon, R.T., Raible, D.W., 1998. Control of neural crest cell fate by the Wnt signalling pathway. Nature 396, 370–373.

Draper, B.W., Morcos, P.A., Kimmel, C.B., 2001. Inhibition of zebrafish fgf8 pre-mRNA splicing with morpholino oligos: a quantifiable method for gene knockdown. Genesis 30, 154–156.

Dutton, K., Dutton, J.R., Pauliny, A., Kelsh, R.N., 2001a. A morpholino phenocopy of the colourless mutant. Genesis 30, 188–189.

Dutton, K.A., Pauliny, A., Lopes, S.S., Elworthy, S., Carney, T.J., Rauch, J., Geisler, R., Haffter, P., Kelsh, R.N., 2001b. Zebrafish colourless encodes sox10 and specifies non-ectomesenchymal neural crest fates. Development 128, 4113–4125.

Fenner, M.H., Parrish, J.E., Boyd, Y., Reed, V., MacDonald, M., Nelson, D.L., Isselbacher, K.J., Shioda, T., 1998. MSG1 (melanocyte-specific gene 1): mapping to chromosome Xq13.1, genomic organization, and promoter analysis. Genomics 51, 401–407.

Furthauer, M., Thisse, C., Thisse, B., 1997. A role for FGF-8 in the dorsoventral patterning of the zebrafish gastrula. Development 124, 4253–4264.

Greco, D., Zellmer, E., Zhang, Z., Lewis, E., 1995. Transcription factor AP-2 regulates expression of the dopamine beta-hydroxylase gene. J. Neurochem. 65, 510–516.

Hilger-Eversheim, K., Moser, M., Schorle, H., Buettner, R., 2000. Regu-

latory roles of AP-2 transcription factors in vertebrate development, apoptosis and cell-cycle control. Gene 260, 1–12.

Hosoda, K., Hammer, R.E., Richardson, J.A., Baynash, A.G., Cheung, J.C., Giaid, A., Yanagisawa, M., 1994. Targeted and natural (piebald-lethal) mutations of endothelin-B receptor gene produce megacolon associated with spotted coat color in mice. Cell 79, 1267–1276.

Huang, S., Jean, D., Luca, M., Tainsky, M.A., Bar-Eli, M., 1998. Loss of AP-2 results in downregulation of c-KIT and enhancement of melanoma tumorigenicity and metastasis. EMBO J. 17, 4358–4369.

Hunter, M.P., Prince, V.E., 2002. Zebrafish hox paralogue group 2 genes function redundantly as selector genes to pattern the second pharyngeal arch. Dev. Biol. 247, 367–389.

Isogai, S., Horiguchi, M., Weinstein, B.M., 2001. The vascular anatomy of the developing zebrafish: an atlas of embryonic and early larval development. Dev. Biol. 230, 278–301.

Ito, M., Kawa, Y., Ono, H., Okura, M., Baba, T., Kubota, Y., Nishikawa, S.I., Mizoguchi, M., 1999. Removal of stem cell factor or addition of monoclonal anti-c-KIT antibody induces apoptosis in murine melanocyte precursors. J. Invest. Dermatol. 112, 796–801.

Kelsh, R.N., Brand, M., Jiang, Y.J., Heisenberg, C.P., Lin, S., Haffter, P., Odenthal, J., Mullins, M.C., van Eeden, F.J., Furutani-Seiki, M., Granato, M., Hammerschmidt, M., Kane, D.A., Warga, R.M., Beuchle, D., Vogelsang, L., Nusslein-Volhard, C., 1996. Zebrafish pigmentation mutations and the processes of neural crest development. Development 123, 369–389.

Kim, H.S., Hong, S.J., LeDoux, M.S., Kim, K.S., 2001. Regulation of the tyrosine hydroxylase and dopamine beta-hydroxylase genes by the transcription factor AP-2. J. Neurochem. 76, 280–294.

Kimmel, C.B., Ballard, W.W., Kimmel, S.R., Ullmann, B., Schilling, T.F., 1995. Stages of embryonic development of the zebrafish. Dev. Dyn. 203, 253–310.

Kimmel, C.B., Miller, C.T., Kruze, G., Ullmann, B., BreMiller, R.A., Larison, K.D., Snyder, H.C., 1998. The shaping of pharyngeal cartilages during early development of the zebrafish. Dev. Biol. 203, 245–263.

Korzh, V., Sleptsova, I., Liao, J., He, J., Gong, Z., 1998. Expression of zebrafish bHLH genes ngn1 and nrd defines distinct stages of neural differentiation. Dev. Dyn. 213, 92–104.

Kunisada, T., Yoshida, H., Yamazaki, H., Miyamoto, A., Hemmi, H., Nishimura, E., Shultz, L.D., Nishikawa, S., Hayashi, S., 1998. Transgene expression of steel factor in the basal layer of epidermis promotes survival, proliferation, differentiation and migration of melanocyte precursors. Development 125, 2915–2923.

Lahav, R., Ziller, C., Dupin, E., Le Douarin, N.M., 1996. Endothelin 3 promotes neural crest cell proliferation and mediates a vast increase in melanocyte number in culture. Proc. Natl. Acad. Sci. U. S. A. 93, 3892–3897.

Le Douarin, N., Kalcheim, K., 1999. The Neural Crest University Press, Cambridge.

Lee, H.O., Levorse, J.M., Shin, M.K., 2003. The endothelin receptor-B is required for the migration of neural crest-derived melanocyte and enteric neuron precursors. Dev. Biol. 259, 162–175.

Li, Y.X., Zdanowicz, M., Young, L., Kumiski, D., Leatherbury, L., Kirby, M.L., 2003. Cardiac neural crest in zebrafish embryos contributes to myocardial cell lineage and early heart function. Dev. Dyn. 226, 540–550.

Limesand, S.W., Anthony, R.V., 2001. Novel activator protein-2alpha splice-variants function as transactivators of the ovine placental lactogen gene. Eur. J. Biochem. 268, 2390–2401.

Lister, J.A., Robertson, C.P., Lepage, T., Johnson, S.L., Raible, D.W., 1999. nacre encodes a zebrafish microphthalmia-related protein that regulates neural-crest-derived pigment cell fate. Development 126, 3757–3767.

Luo, R., An, M., Arduini, B.L., Henion, P.D., 2001. Specific pan-neural crest expression of zebrafish Crestin throughout embryonic development. Dev. Dyn. 220, 169–174.

Luo, T., Matsuo-Takasaki, M., Thomas, M.L., Weeks, D.L., Sargent, T.D., 2002. Transcription factor AP-2 is an essential and direct regulator of epidermal development in *Xenopus*. Dev. Biol. 245, 136–144.

Luo, T., Lee, Y.H., Saint-Jeannet, J.P., Sargent, T.D., 2003. Induction of neural crest in *Xenopus* by transcription factor AP2alpha. Proc. Natl. Acad. Sci. U. S. A. 100, 532–537.

Maconochie, M., Krishnamurthy, R., Nonchev, S., Meier, P., Manzanares, M., Mitchell, P.J., Krumlauf, R., 1999. Regulation of Hoxa2 in cranial neural crest cells involves members of the AP-2 family. Development 126, 1483–1494.

Marusich, M.F., Furneaux, H.M., Henion, P.D., Weston, J.A., 1994. Hu neuronal proteins are expressed in proliferating neurogenic cells. J. Neurobiol. 25, 143–155.

Mazina, O.M., Phillips, M.A., Williams, T., Vines, C.A., Cherr, G.N., Rice, R.H., 2001. Redistribution of transcription factor AP-2alpha in differentiating cultured human epidermal cells. J. Invest. Dermatol. 117, 864–870.

McPherson, L.A., Baichwal, V.R., Weigel, R.J., 1997. Identification of ERF-1 as a member of the AP2 transcription factor family. Proc. Natl. Acad. Sci. U. S. A. 94, 4342–4347.

Meier, P., Koedood, M., Philipp, J., Fontana, A., Mitchell, P.J., 1995. Alternative mRNAs encode multiple isoforms of transcription factor AP-2 during murine embryogenesis. Dev. Biol. 169, 1–14.

Metcalfe, W.K., Myers, P.Z., Trevarrow, B., Bass, M.B., Kimmel, C.B., 1990. Primary neurons that express the L2/HNK-1 carbohydrate during early development in the zebrafish. Development 110, 491–504.

Meulemans, D., Bronner-Fraser, M., 2002. Amphioxus and lamprey AP-2 genes: implications for neural crest evolution and migration patterns. Development 129, 4953–4962.

Mitchell, P.J., Timmons, P.M., Hebert, J.M., Rigby, P.W., Tjian, R., 1991. Transcription factor AP-2 is expressed in neural crest cell lineages during mouse embryogenesis. Genes Dev. 5, 105–119.

Moser, M., Pscherer, A., Bauer, R., Imhof, A., Seegers, S., Kerscher, M., Buettner, R., 1993. The complete murine cDNA sequence of the transcription factor AP-2. Nucleic Acids Res. 21, 4844.

Moser, M., Imhof, A., Pscherer, A., Bauer, R., Amselgruber, W., Sinowatz, F., Hofstadter, F., Schule, R., Buettner, R., 1995. Cloning and characterization of a second AP-2 transcription factor: AP-2 beta. Development 121, 2779–2788.

Moser, M., Ruschoff, J., Buettner, R., 1997. Comparative analysis of AP-2 alpha and AP-2 beta gene expression during murine embryogenesis. Dev. Dyn. 208, 115–124.

Nair, S.S., Chaubal, V.A., Shioda, T., Coser, K.R., Mojamdar, M., 2001. Over-expression of MSG1 transcriptional co-activator increases melanin in B16 melanoma cells: a possible role for MSG1 in melanogenesis. Pigment Cell Res. 14, 206–209.

Nasevicius, A., Ekker, S.C., 2000. Effective targeted gene 'knockdown' in zebrafish. Nat. Genet. 26, 216–220 (taf/DynaPage.taf?file=/ng/journal/v26/n2/full/ng1000_216.html, taf/DynaPage.taf?file=/ng/journal/v26/n2/abs/ng1000_216.html).

Nguyen, V.H., Schmid, B., Trout, J., Connors, S.A., Ekker, M., Mullins, M.C., 1998. Ventral and lateral regions of the zebrafish gastrula, including the neural crest progenitors, are established by a bmp2b/swirl pathway of genes. Dev. Biol. 199, 93–110.

Nocka, K., Majumder, S., Chabot, B., Ray, P., Cervone, M., Bernstein, A., Besmer, P., 1989. Expression of c-kit gene products in known cellular targets of W mutations in normal and W mutant mice-evidence for an impaired c-kit kinase in mutant mice. Genes Dev. 3, 816–826.

Nocka, K., Tan, J.C., Chiu, E., Chu, T.Y., Ray, P., Traktman, P., Besmer, P., 1990. Molecular bases of dominant negative and loss of function mutations at the murine c-kit/white spotting locus: W37, Wv, W41 and W. EMBO J. 9, 1805–1813.

Nottoli, T., Hagopian-Donaldson, S., Zhang, J., Perkins, A., Williams, T., 1998. AP-2-null cells disrupt morphogenesis of the eye, face, and limbs in chimeric mice. Proc. Natl. Acad. Sci. U. S. A. 95, 13714–13719.

Odenthal, J., Nusslein-Volhard, C., 1998. Fork head domain genes in zebrafish. Dev. Genes Evol. 208, 245–258.

Oyama, N., Takahashi, H., Tojo, M., Iwatsuki, K., Iizuka, H., Nakamura, K., Homma, Y., Kaneko, F., 2002. Different properties of three isoforms (alpha, beta, and gamma) of transcription factor AP-2 in the expression of human keratinocyte genes. Arch. Dermatol. Res. 294, 273–280.

Parichy, D., Rawls, J.F., Pratt, S.J., Whitfield, T.T., Johnson, S.L., 1999. Zebrafish sparse corresponds to an orthologue of c-kit and is required for morphogenesis of a subpopulation of melanocytes, but is not essential for hematopoiesis or primordial germ cell development. Development 126, 3425–3436.

Parichy, D.M., Mellgren, E.M., Rawls, J.F., Lopes, S.S., Kelsh, R.N., Johnson, S.L., 2000a. Mutational analysis of endothelin receptor b1 (rose) during neural crest and pigment pattern development in the zebrafish *Danio rerio*. Dev. Biol. 227, 294–306.

Parichy, D.M., Ransom, D.G., Paw, B., Zon, L.I., Johnson, S.L., 2000b. An orthologue of the kit-related gene fms is required for development of neural crest-derived xanthophores and a subpopulation of adult melanocytes in the zebrafish, *Danio rerio*. Development 127, 3031–3044.

Passarge, E., 2002. Dissecting Hirschsprung disease. Nat. Genet. 31, 11–12.

Pawelek, J.M., Chakraborty, A.K., 1998. The enzymology of melanogenesis. In: Nordlund, J.J., Boissy, R.E., Hearing, B.J., King, R.A., Ortonne, J.-P. (Eds.), The Pigmentary System. Oxford Univ. Press, New York.

Prescott, N.J., Lees, M.M., Winter, R.M., Malcolm, S., 2000. Identification of susceptibility loci for nonsyndromic cleft lip with or without cleft palate in a two stage genome scan of affected sib-pairs. Hum. Genet. 106, 345–350.

Reid, K., Turnley, A.M., Maxwell, G.D., Kurihara, Y., Kurihara, H., Bartlett, P.F., Murphy, M., 1996. Multiple roles for endothelin in melanocyte development: regulation of progenitor number and stimulation of differentiation. Development 122, 3911–3919.

Reith, A.D., Rottapel, R., Giddens, E., Brady, C., Forrester, L., Bernstein, A., 1990. W mutant mice with mild or severe developmental defects contain distinct point mutations in the kinase domain of the c-kit receptor. Genes Dev. 4, 390–400.

Rubinstein, A.L., Lee, D., Luo, R., Henion, P.D., Halpern, M.E., 2000. Genes dependent on zebrafish cyclops function identified by AFLP differential gene expression screen. Genesis 26, 86–97.

Scapoli, L., Pezzetti, F., Carinci, F., Martinelli, M., Carinci, P., Tognon, M., 1997. Evidence of linkage to 6p23 and genetic heterogeneity in nonsyndromic cleft lip with or without cleft palate. Genomics 43, 216–220.

Schilling, T.F., Piotrowski, T., Grandel, H., Brand, M., Heisenberg, C.P., Jiang, Y.J., Beuchle, D., Hammerschmidt, M., Kane, D.A., Mullins, M.C., van Eeden, F.J., Kelsh, R.N., Furutani-Seiki, M., Granato, M., Haffter, P., Odenthal, J., Warga, R.M., Trowe, T., Nusslein-Volhard, C., 1996. Jaw and branchial arch mutants in zebrafish I: branchial arches. Development 123, 329–344.

Schorle, H., Meier, P., Buchert, M., Jaenisch, R., Mitchell, P.J., 1996. Transcription factor AP-2 essential for cranial closure and craniofacial development. Nature 381, 235–238.

Shim, W.K., Derieg, M., Powell, B.R., Hsia, Y.E., 1999. Near-total intestinal aganglionosis in the Waardenburg–Shah syndrome. J. Pediatr. Surg. 34, 1853–1855.

Shin, M.K., Levorse, J.M., Ingram, R.S., Tilghman, S.M., 1999. The temporal requirement for endothelin receptor-B signalling during neural crest development. Nature 402, 496–501.

Steel, K.P., Davidson, D.R., Jackson, I.J., 1992. TRP-2/DT, a new early melanoblast marker, shows that steel growth factor (c-kit ligand) is a survival factor. Development 115, 1111–1119.

Stewart, H.J., Brennan, A., Rahman, M., Zoidl, G., Mitchell, P.J., Jessen, K.R., Mirsky, R., 2001. Developmental regulation and overexpression of the transcription factor AP-2, a potential regulator of the timing of Schwann cell generation. Eur. J. Neurosci. 14, 363–372.

Tachibana, M., 2000. MITF: a stream flowing for pigment cells. Pigment Cell Res. 13, 230–240.

Tan, J.C., Nocka, K., Ray, P., Traktman, P., Besmer, P., 1990. The dominant W42 spotting phenotype results from a missense mutation in the c-kit receptor kinase. Science 247, 209–212.

Voisey, J., van Daal, A., 2002. Agouti: from mouse to man, from skin to fat. Pigment Cell Res. 15, 10–18.

Wankhade, S., Yu, Y., Weinberg, J., Tainsky, M.A., Kannan, P., 2000. Characterization of the activation domains of AP-2 family transcription factors. J. Biol. Chem. 275, 29701–29708.

Westerfield, M., 1993. The Zebrafish Book University of Oregon Press, Eugene, OR.

Williams, T., Admon, A., Luscher, B., Tjian, R., 1988. Cloning and expression of AP-2, a cell-type-specific transcription factor that activates inducible enhancer elements. Genes Dev. 2, 1557–1569.

Winning, R.S., Shea, L.J., Marcus, S.J., Sargent, T.D., 1991. Developmental regulation of transcription factor AP-2 during *Xenopus laevis* embryogenesis. Nucleic Acids Res. 19, 3709–3714.

Yang, C., Kim, H.S., Seo, H., Kim, K.S., 1998. Identification and characterization of potential *cis*-regulatory elements governing transcriptional activation of the rat tyrosine hydroxylase gene. J. Neurochem. 71, 1358–1368.

Zhang, J., Hagopian-Donaldson, S., Serbedzija, G., Elsemore, J., Plehn-Dujowich, D., McMahon, A.P., Flavell, R.A., Williams, T., 1996. Neural tube, skeletal and body wall defects in mice lacking transcription factor AP-2. Nature 381, 238–241.

Zhao, F., Satoda, M., Licht, J.D., Hayashizaki, Y., Gelb, B.D., 2001. Cloning and characterization of a novel mouse AP-2 transcription factor, AP-2delta, with unique DNA binding and transactivation properties. J. Biol. Chem. 276, 40755–40760.

Electronic resources

Online Mendelian Inheritance in Man, OMIM (TM). Johns Hopkins University, Baltimore, MD. MIM Number: 119530: 03/06/03; 169100: 01/31/02. World Wide Web URL: http://www.ncbi.nlm.nih.gov/omim/, http://www.ncbi.nlm.nih.gov/, http://www.ensembl.org.